Terpenoids for medicine

Fischedick, J.

Chapter 5

Activation of antioxidant response element in mouse primary cortical cultures with sesquiterpene lactones isolated from *Tanacetum parthenium*

Justin T Fischedick[a,b], Miranda Standiford[c], Delinda A. Johnson[c], Ric C.H. De Vos[d,e,f], Slađana Todorović[g], Tijana Banjanac[g], Rob Verpoorte[b], Jeffrey A. Johnson[c]

[a] *PRISNA BV, Einsteinweg 55, 2300 RA Leiden, The Netherlands*
[b] *Natural Products Laboratory, Institute of Biology, Leiden University, 2300 RA Leiden, The Netherlands*
[c] *Division of Pharmaceutical Sciences, School of Pharmacy, University of Wisconsin, Madison, WI, USA*
[d] *Plant Research International, BU Biosciences, Wageningen University and Research Centre, Wageningen, The Netherlands*
[e] *Centre for BioSystems Genomics, Wageningen, The Netherlands*
[f] *Netherlands Metabolomics Centre, Leiden, The Netherlands*
[g] *Institute for Biological Research "Siniša Stanković", University of Belgrade, Belgrade, Serbia*

Abstract

Tanacetum parthenium (Asteraceae) produces biologically active sesquiterpene lactones (SL). Nuclear factor E2-related factor 2 (Nrf2) is a transcription factor known to activate a series of genes termed the antioxidant response element (ARE). Activation of Nrf2/ARE may be useful for the treatment of neurodegenerative disease. In this study we isolated 11 SL from *T. parthenium* with centrifugal partition chromatography and semi-preparative HPLC. Compounds were screened *in-vitro* for their ability to activate the ARE on primary mouse cortical cultures as well as for their toxicity towards the cultures. All SL containing the α-methylene-γ-lactone moiety were able to activate the ARE and cause cellular toxicity. The structure activity relationship among the SL isolated indicates that the guaianolides were more active and when lacking the endoperoxide functionality less toxic then the germacranolides.

Published:

Fischedick, J., Standiford, M., Johnson, D., De Vos, R., Todorović, S., Banjanac, T., Verpoorte, R., Johnson, J., 2012. Activation of Antioxidant Response Element in Mouse Primary Cortical Cultures with Sesquiterpene Lactones Isolated from *Tanacetum parthenium*. Planta Medica 78, 1725–1730.

Introduction

Tanacetum parthenium L. (syn. *Chrysanthemum parthenium*), commonly known as feverfew, is a member of the Asteraceae family containing various sesquiterpene lactones (SL) from the germacranolide, eudesmanolide, and guaianolide groups. In European traditional medicine, *T. parthenium* has been used for the treatment of migraine and rheumatism. The germacranolide, 4α,5β-epoxy-germacra-1-(10),11-(13)-dien-12,6α-olide (parthenolide (**1**)) is often regarded as the primary active ingredient in *T. parthenium* (Abed et al., 1995). Parthenolide exhibits numerous biological activities such as cytotoxicity, anti-viral, anti-leishmanial, and anti-inflammatory action (Hwang et al., 2006; Tiuman et al., 2005; Salminen et al., 2008). In past decades **1** and other SL have been the subject of cancer clinical trials (Ghantous et al., 2010).

Nrf2 is a transcription factor known to induce genes encoding cytoprotective and antioxidant enzymes by binding to the cis-acting enhancer element called ARE, in the promoter of these genes. Activation of Nrf2/ARE pathway with small molecules is a potential strategy to treat neurodegenerative diseases (Calkins et al., 2009; de Vries et al., 2008). Nrf2 localization and degradation is regulated by its cytoplasmic repressor protein the Kelch-like ECH-associated protein 1 (Keap1). Various compounds or reactive oxygen species (ROS) can interfere with the ability of Keap1 to bind Nrf2 and thereby up-regulate activation of ARE (de Vries et al., 2008). A series of conserved cysteine residues on Keap1 are important for compounds like tert-buytlhydroxyquinone (*t*BHQ) or ROS to liberate Nrf2 from Keap1 (Zhang and Hannink, 2003; Itoh et al., 2004).

The biological activity of many SL such as **1** is often attributed to the presence of the α-methylene-γ-lactone moiety. The nucleophilic methylene can react with biological thiols, such as cysteine residues on proteins, by a Michael addition type reaction (Mathema et al., 2012). Mild activation of Nrf2/ARE by **1** has been demonstrated using human hepatoma (HepG2) cells and SL from *Calea urticifolia* along with **1** in rat pheochromocytoma (PC12) cells (Jeong et al., 2005; Umemura et al., 2008). Neither study however investigated 11,13-dihydro versions of the compounds to confirm importance of α-methylene-γ-lactone moiety nor the toxicity of **1**. Another study demonstrated a neuroprotective effect of the SL isoatriplicolide tiglate against glutamate induced toxicity on primary rat cortical cells, however molecular mechanisms and toxicity were not investigated (Kim et al., 2010). Neurotoxic effects of SL such as repin from *Centaurea* species, which causes a disease in horses called equine nigropallidal enchalomalacia, have also been reported (Tukov et al., 2004).

Therefore in order to gain further insight into the structure activity relationships of SL for Nrf2/ARE activation, a variety of SL were isolated from *T. parthenium*. Due to difficulties reported in the isolation of certain SL from *T. parthenium* (Bohlmann and Zdero, 1982), a centrifugal partition chromatography (CPC) method was developed to improve their isolation. Isolated compounds were screened *in vitro* for ARE activation using primary mouse cortical cultures derived from ARE-human placental alkaline phosphatase (hPAP) transgenic reporter mice (Johnson et al.,

2002). Since SL are potentially neurotoxic, the compounds toxicity towards the cultures was also evaluated using the 3-(4,5-dimethylthiazol-2-yl)-5-(3-carboxymethoxyphenyl)-2-(4-sulfophenyl) 2H tetrazoluim inner salt (MTS) assay.

Materials and Methods

Chemicals

Ethylacetate (EtOAc), n-heptane (Hept), methanol (MeOH), ethanol (EtOH), n-hexane (Hex), diethylether (Et_2O), acetone, dichloromethane (DCM) of analytical reagent grade, and MeOH HPLC grade were purchased from Biosolve BV (Valkenswaard, The Netherlands). Et_2O was distilled at 35 °C prior to use. Vanillin, parthenolide (90% purity), and chloroform ($CHCl_3$) were from Sigma-Aldrich Inc. (St. Louis, Missouri, USA). Sulfuric acid 95-97% from Fluka GmbH (Buchs, Switzerland), magnesium sulfate ($MgSO_4$) from Brocacef BV (Maarssen, The Netherlands), silica gel 60 (0.063 - 0.2 mm) for column chromatography, and silica gel 60 F_{254} 10 x 20 cm TLC plates (Merck, Darmstadt, Germany) were used. $CDCl_3$ was purchased from Eurisotop SA (Gif-Sur-Yvette, France).

Plant material

One kg of the dried aerial parts of *T. parthenium* was purchased from De Groene Luifel BV (Sluis, The Netherlands) referred to as NL and 2 kg of the dried flower heads of *T. parthenium* was grown at the University of Belgrade Institute for Biological Research referred to as IBRSS. Plant material was identified by Wout Holverda and voucher specimens were deposited in the economic botany collection of the National Herbarium Nederland in Leiden under the following barcodes 0991399 J. Fischedick No. 132010 and 0991384 J. Fischedick No. 172010.

Crude extraction preparation

Two hundred and fifty g of NL plant material was extracted 3 times with 4, 3, and 3 L of EtOH with stirring for 24 h each with an initial 30 min of ultra-sonication. EtOH extracts were combined and solvent removed under reduced pressure at 40 °C. The extract was then dissolved in 500 mL EtOAc and rinsed 3 times with 500 mL H_2O. The EtOAc fraction was dried over $MgSO_4$, filtered, and EtOAc removed under reduced pressure at 40 °C yielding 8.0 g of a dark green extract (Extract 1). Extract 2 was prepared in the same way as extract 1 except 250 g of IBRSS plant material, flower heads only, was used and yielded 17.3 g of a dark golden extract.

CPC apparatus and solvent system selection

CPC experiments were carried out on a Fast Centrifugal Partition Chromatograph with a 1 L internal volume rotor (Kromaton Technologies, Angers, France). The CPC was connected to a Rheodyne injector equipped with a 30 mL injection loop (Rheodyne Inc, Cotati, CA, USA), an AP100 Armen instruments pump (Saint-Avé, France), and a LKB Bromma Fraction Collector 2211 SuperRac (Bromma, Sweden). A Tamson Instruments BV (Bleiswijk, The Netherlands) Low Temperature

Circulator TLC15 set at 21 °C was used to maintain a constant temperature inside the rotor chamber. The CPC solvent system was selected by screening 3 and 4 solvent bi-phasic mixtures described in (Foucault, 1995) for the ability to solubilize a crude *T. parthenium* extract and evenly partition compounds between the upper (↑) and lower (↓) layers. Partitioning of compounds was assessed visually by TLC ($CHCl_3$: EtOAc; 7: 3; vanillin/sulfuric acid reagent) analysis of ↑ and ↓ layers. Finally a solvent system composed of Hept: EtOAc: MeOH: H_2O, 1:1:1:1 (HEMW) solvent system was selected for fractionation of extract 1 and 2.

CPC experiments

Extract 1 could be dissolved in 90 mL of 1:1 mixture of ↑:↓ layer of the HEMW system while extract 2 could be dissolved in 110 mL. In total six CPC experiments were performed to process extracts 1 (CPC1-3) and 2 (CPC4-6). Each CPC experiment consisted of the following procedure. Four L HEMW was prepared by mixing for 1 h, settling for 1 h, and separating into ↑ and ↓ layer. Initially 1.1 L of the ↓ layer was pumped into the CPC system to act as the stationary phase. The CPC was equilibrated by pumping the ↑ layer in ascending mode, at a flow rate of 10 mL/min, and rotor speed of 1000 rpm. The system was in equilibrium when the ↑ layer began to elute and the volume of ↓ layer displaced was recorded (void volume). Thirty mL of sample was injected for all experiments except for experiment 6 which was 50 mL. The 50 mL injection was performed by first injecting 30 mL of the sample, allowing 10 mL/min flow rate to run for 3 min, flow stopped while remaining 20 mL of sample was injected, and the run was continued as normal.

Initially during each CPC experiment 400 mL of the eluent was collected in a glass bottle (FrI) then 85 x 10 mL fractions (Fr) were collected in glass test tubes. After the 85^{th} fraction was collected the ↓ layer was pumped into the system. The remaining ↑ layer was collected in a glass bottle and the fraction labeled Fr↑. Finally 800 mL of the ↓ layer was eluted and this fraction labeled Fr↓. Some ↓ layer bleeding was observed in each experiment however it was confined to FrI. Fractions were analyzed by TLC in the same way as above and combined based on similarity of chemical profile.

HPLC

An Agilent 1200 series HPLC was used for analyzing purity of combined fractions and isolated compounds. The system consisted of a G1322A degasser, G1311A quaternary pump, G1367B Hip automated liquid sampler, and G1315D diode-array (DAD) detector (Agilent technologies Inc, Santa Clara, CA, USA). The software used was Chemstation Rev. B03.02. A 150 x 4.6 mm Luna 5 micron C18 (2) 100A column equipped with a guard column containing C18 4 x 3 mm cartridges was used for separation (Phenomenex Inc, Torrance, CA, USA). Gradient elution with a flow of 0.5 mL/min consisted initially of 50% H_2O and 50% MeOH which increased to 100% MeOH over 40 min and remained at 100% MeOH for 10 min. The DAD detector was set at 210 nm with a UV spectrum scan from 190-390 nm.

Semi-preparative HPLC general procedure

Semi-preparative HPLC (pHPLC) was performed with 2 LC-10ADvp liquid chromatograph pumps, a SPD-10Avp UV-vis detector, a SCL-10Avp system controller, a FRC-10A Fraction Collector, and controlled by software LCsolution Version 1.21 SP1 all manufactured by Shimadzu (Kyoto, Japan). A Luna C18 (2) 100 A 5 micron 250 x 10 mm column was used for reverse phase pHPLC (RP) and a Luna Silica (2) 100 A 5 micron 250 x 10 mm column equipped with a security guard cartridge holder (10 mm internal diameter) containing a security guard semiprep cartridge silica (10 x 10 mm) was used for normal phase pHPLC (NP) (Phenomenex, Torrance, CA, USA). Flow rates were 5 mL/min, UV 210 and 254 nm, and 10 mL fractions were collected. After filtration over a 25 mm 0.45 µm PTFE syringe filter samples were injected manually into the pHPLC system using a Rheodyne injector equipped with a 5 mL injection loop. NP samples were dissolved in 5 mL DCM for injection. After each NP experiment column was rinsed with 100 mL of acetone or EtOAc (rinse fraction) and fractions were combined based on similarity of TLC profile. RP samples were dissolved in 1-5 mL mobile phase or pure MeOH. RP fractions were combined based on UV chromatograms, MeOH removed under reduced pressure at 40 °C, remaining H_2O frozen at -20 °C, and sample lyophilized to dryness.

Purification

CPC experiments 1-3 Fr_{43-70} (540 mg) was fractionated by NP (Hept: EtOAc, 9:1). Fr_{13-26} were combined and solvent removed to yield of **1 (**408 mg, 96% pure) as a clear gum which can be crystallized to white needles using cyclohexane. Fr_{27-33} (11 mg) was further purified with RP (H_2O: MeOH, 1:1, isocratic) yielding 11,13-dihydroparthenolide (**2**) (4.9 mg, >99%). CPC 1-3 Fr_{71-85} (55 mg) was fractionated by NP (Hept: EtOAc, gradient) with Fr_{29} (1.9 mg) and Fr_{44} (0.8 mg) being purified with RP (H_2O: MeOH, 1:1, isocratic) yielding anhydroverlotorin (**3**) (0.2 mg, 82%) and santamarine (**4**) (0.4 mg, >99%) respectively. CPC 1-3 Fr↑ (78 mg) was fractionated by NP (Hept: EtOAc, gradient) with Fr_7 being purified with RP (H2O: MeOH, 3:7, isocratic) yielding **3** (0.8 mg, 87%) and Fr_{34-35} (0.4 mg) purified with RP (H2O: MeOH, 1:1, isocratic) yielding reynosin (**5**) (0.3 mg, 88%). CPC 1-3 Fr↓ (2.2 g) was fractionated with an additional CPC experiment (7) using a 200 mL rotor, HEMW 4:6:4:6 solvent system, with all other CPC conditions same as described above. Seventy 10 mL fractions were collected. CPC 7 fractions Fr_{10-20} (508 mg), Fr_{21-42} (506 mg), Fr_{43-50} (78 mg), and Fr_{51-70} (130 mg) were each further separated by NP (Hept: EtOAc, 7:3) with subsequent fractions being purified with repeated RP to yield 3β-hydroxycostunolide (**6**) (4.8 mg, 94%), costunolide diepoxide (**7**) (13 mg, 90%), 3-hydroxyparthenolide (**8**) (20.2 mg, 94%), artemorin (**9**) (4.6 mg, 98%), and artecanin (**10**) (1.1 mg, 95%).

CPC 4-6 Fr_{40-70} was dissolved in 30 mL EtOAc, loaded onto 10 g of silica gel, eluted with 200 mL EtOAc, and solvent removed to yield **1** (2.3 g, 98%), which was crystallized from Et_2O: Hex to white/yellow needles. CPC 4-6 Fr_{71-85} and Fr↑ were combined (490 mg) and separated with NP (Hept: EtOAc, gradient) with Fr_{15-16} (44 mg) and Fr_{22-24} (22 mg) further purified with RP (H_2O: MeOH, gradient) to yield **3** (1.5 mg, 99%) and **6** (3.6 mg, 74%) respectively. CPC 4-6 Fr↓ (4 g) was separated by flash chromatography (150 g silica) using Hex with increasing proportion EtOAc followed by

EtOAc with increasing proportions of acetone into 17-100 mL fractions. Flash Fr_{8-9} (434 mg) was further purified with repeated RP to yield **8** (1.7 mg, 90%), **6** (27.5 mg, 86%), and tanaparthin-β-peroxide (**11**) (3.9 mg, 76%). Flash Fr_{10-17} (2.6 g) was again fractionated by flash chromatography (100 g silica) using Hex with increasing proportion of acetone. Subsequent fractions were purified with repeated RP to yield **7** (18 mg, 99%), **10** (13.3 mg, 82%), **9** (32.1 mg, 96%), and **11** (2.3 mg, 87%).

Structure elucidation

^{1}H-NMR and COSY spectra were acquired on a Bruker DMX 500 MHz NMR (Karlsruhe, Germany). The solvent was $CDCl_3$ and chemical shift was calibrated to residual solvent (7.26 ppm). High resolution mass spectrometry was performed on an LC-LTQ-Orbitrap FTMS system (Thermo Scientific, Waltham, Massachusetts, USA). The instrument consisted of an Accela HPLC, an Accela photodiode array detector, connected to a LTQ/Orbitrap hybrid mass spectrometer equipped with an ESI source. Chromatographic separation took place on a Phenomenex Luna C18(2) analytical column (150 x 2.0 mm, 3 µm particle size), using H_2O and acetonitrile, both containing 0.1 % v/v formic acid, at a flow rate of 0.19 mL/min and a column temperature at 40 °C. A linear gradient from 5 to 75% acetonitrile in 45 min was applied, which was followed by 15 min of washing and equilibration. FTMS full scans (*m/z* 100−1200) were recorded with a resolution of 60.000, whereas for MS^n scans a resolution of 15.000 was used. The FTMS was externally calibrated in negative mode using sodium formate clusters in the range *m/z* 150-1200 and automatic tuning was performed on *m/z* 384.93.

Primary Cortical Neuronal Cultures

Cultures were derived from ARE-hPAP reporter mice as previously described (Johnson et al., 2002; Kraft et al., 2004). Briefly, cortices from E15 mouse pups were pooled in 10 mL ice-cold Ca^{2+} and Mg^{2+} free HBSS (Life Technologies, Carlsbad, CA, USA). Tissue was minced, centrifuged and digested in 0.05% trypsin without EDTA in HBSS for 15 min at 37 °C. Following trypsinization, cells were rinsed 3 times with HBSS. Cells were then washed with CEMEM (minimum essential media with Earle's salts; (Life Technologies), 2 mM glutamine, 1% penicillin/streptomycin, and 10% each of heat inactivated fetal bovine serum and horse serum (Atlanta Biologicals, Inc., Lawrenceville, GA, USA) and triturated to a single-cell suspension and strained through a 70 µM cell strainer (BD Biosciences, San Jose, CA, USA). Cells were counted, assayed for viability using trypan blue, and plated at a density of 3 x 105 cell/cm^2 on poly-D-lysine coated plates. Cells were maintained in CEMEM for 45 min, followed by a medium change with CEMEM. After two days, medium was changed from CEMEM to NBM (Neurobasal media; Life Technologies) supplemented with B27 with antioxidants and 2 mM glutamine. These mixed cultures (~ 40% astrocytes and 60% neurons), were left for at least 48 hours in NBM prior to initiating experiments. Cells were incubated at 37 °C in a tri-gas incubator with 5% O_2, 5% CO_2, and 90% N_2.

Compounds were dissolved in 100% DMSO and administered to cells for 48 hours (final concentration of DMSO was 0.1%) after 6 days in culture. Nrf2 activation was determined by measuring for hPAP activity. The hPAP activity assay has been

described previously (Kraft et al., 2004). Briefly, cells were lysed in TMNC lysis buffer (50 mM Tris, 5 mM $MgCl_2$, 100 mM NaCl, 1% 3-[(3-cholamidopropyl)dimethylammonio]-1-propanesulfonate (CHAPS)) and freeze-thawed at -20 ^oC. Extracts were incubated with 200 mM diethanolamine (DEA) buffer at 65 ^oC to inactivate endogenous alkaline phosphatase activity. hPAP activity was quantified in 200 mM DEA with 0.8 mM CSPD [disodium 3-(4-methoxyspiro (1,2-dioxetane-3,2'-(5'-chloro)tricycle(3.3.1.1^{3,7})decan)-4-yl)phenyl phosphate) (Life technologies), 2x Emerald and 5 mM $MgCl_2$]. Luminescence was measured on a Berthold Orion microplate luminometer with one-second integration. Baseline signal from hPAP negative control culture samples was subtracted from all values. Cell viability was assayed using the MTS (3-(4,5-Dimethylthiazol-2-yl)-5-(3-carboxymethoxyphenyl)-2-(4-sulfophenyl)-2H-tetrazolium salt) assay from Promega (Madison, WI, USA) following the manufacturer's suggested protocol.

Statistical analysis

All data are represented as mean ± SEM (n = 5). Statistical analysis was performed using one-way ANOVA followed by Newman-Keuls multiple comparison (GraphPad prism version 4).

Appendix

Detailed *T. parthenium* growth conditions, NMR data, and high resolution MS, are available in chapter 5 appendix.

Results and Discussion

For CPC experiments the void volume ranged from 210-250 mL and the pressure ranged from 51-57 bar between runs. Up to 7.9 g of extract 2 could be injected without destabilizing the CPC system while maintaining a good separation of **1**. Compound **1** eluted in similar fractions between NL and IBRSS plant material. These results indicate that the CPC method is robust and reproducible for the isolation of **1**. IBRSS flower heads of *T. parthenium* yielded higher amounts of **1** (0.9% dry weight) then NL material which can be explained by observations that **1** accumulates mostly in the flower heads compared to other plant parts (Majdi et al., 2011). With CPC the yields of **1** from IBRSS material are higher then those using low pressure or open column chromatography with silica (Bohlmann and Zdero, 1982; Milbrodt et al., 1997; Rey et al., 1992). In total 11 SL were isolated (Figure 1). All compounds were identified based on ^{1}H-NMR comparison with literature, COSY, and high resolution MS (Bohlmann and Zdero, 1982; El-Feraly and Chan, 1978; Parodi et al., 1989; Sanz et al., 1989; Romo De Vivar and Jiménez 1965; Yoshioka et al., 1970; Asakawa et al., 1981; El-Feraly and Chan, 1977; Geissman, 1970; Begley et al., 1989).

The purest samples of each SL were selected for hPAP assay (Figure 2) and MTS assay (Figure 3). Compound **2** lacks the α-methylene-γ-lactone moiety and did not increase hPAP levels, while all other SL displayed some level of significant activation confirming the importance of this functional group. Compounds **4**, **5**, **6**, and **10** showed

a linear dose response, although they were weaker compared to the positive control *t*BHQ. Compounds **1**, **7**, **8**, and **9** at higher doses decreased or eliminated activation. This observation can be explained by the MTS results for **1**, **7**, **8**, and **9** which show increasing cellular toxicity at increasing doses (Figure 3A).

Figure 1. Structures of isolated SL. Germacranolides - **1**, **2**, **3**, **6**, **7**, **8**, **9**; eudesmanolides - **4**, **5**; guaianolides – **10**, **11**.

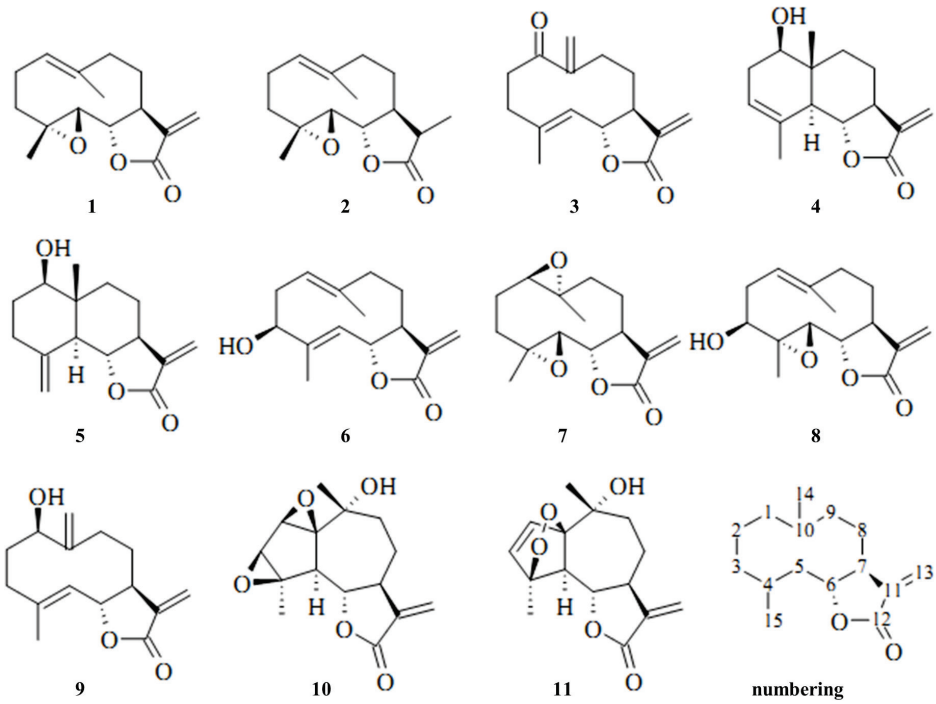

Compounds **3** and **11** at 12.5 µM had nearly 100 fold and >200 fold hPAP activation respectively with considerable toxicity at higher doses (data not shown). Therefore both compounds were assayed at lower doses until a linear dose response was observed and toxicity was lowered (Figure 2B and Figure 3B). Both the α-methylene-γ-lactone and endoperoxide moieties are present in **11**. The related compound **10,** which lacks the endoperoxide group but contains 2 epoxides, had weaker hPAP activity suggesting that the endoperoxide also contributes to the activity of **11**. The potent compound **3** had 2 exocyclic methylene groups at C-11,13 and C-10,14 neighboring a carbonyl. The replacement of the carbonyl with a hydroxyl group at position 1 as in **9** weakens activity. The presence of an extra methylene group could provide an additional reactive alkylating center in the molecule leading to more activity. Similar observations were reported in a previous study (Umemura et al., 2008).

Figure 2. Fold increase in hPAP luminescence over negative controls. *Statistically significant increase, $p < 0.05$.

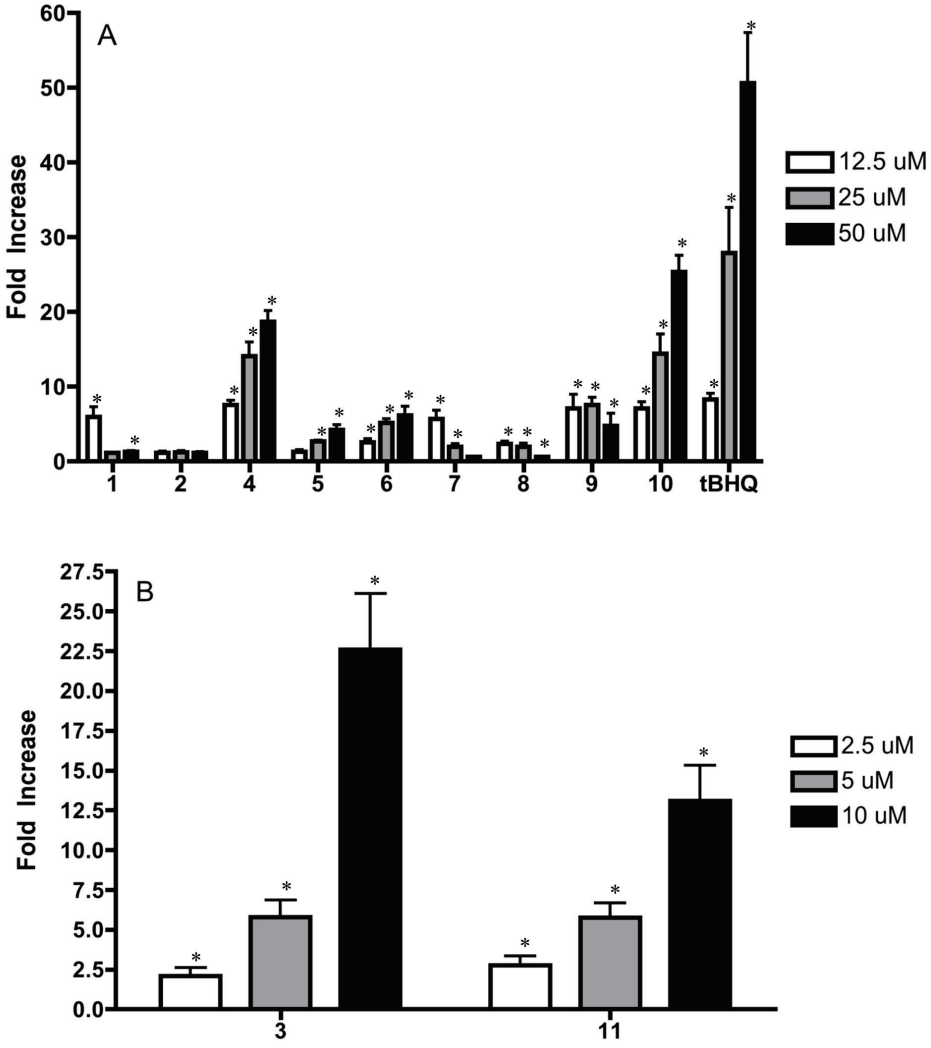

A common structural feature for the germacranolides **1**, **7**, and **8** is the presence of epoxides at positions 4 and 5 as well as 1 and 10 in the case of **7.** Compounds **1**, **7**, and **8** were among the most toxic compounds in the MTS assay and had both low and non-linear activity in the hPAP assay. Elimination of the epoxide as in **6,** eliminated toxicity at 5 and 12.5 μM and reduced it at 50 μM when compared with **1**, **7**, and **8** confirming the importance of epoxide functionality for toxicity. The guaianolide **10** also contains epoxide groups, however it is the least toxic of the most active SL's containing α-methylene-γ-lactone moiety, with a potency of about half that of *t*BHQ. This suggests that the differences between the open, germacranolide ring and

the bridged, guaianolide ring plays an important role in the activity of these compounds. Lewis-acid catalyzed intramolecular cyclization reactions of germanacranolides into guaianolides are known to occur (Castaneda-Acosta and Fischer, 1993; Parodi et al., 1989). Other biological activities such as anti-cancer activity and anti-inflammatory action are known to differ between various SL skeletons (Ghantous et al., 2010; Neukirch et al., 2003). Whether or not intramolecular cyclizations of germacranolides to guaianolides occur *in-vivo* is worth further investigation. With regards to the eudesmanolides **4** and **5**, these compounds could only be isolated in very low amounts and therefore we were unable to fully evaluate their toxicity (Figure 3A). Compound **4** was the second most potent germacranolide for hPAP activation (Figure 2A), although even at low doses toxicity was observed (Figure 3A). Compound **5** mildly stimulated hPAP activation and no toxicity was observed at the doses tested.

From these results, we can conclude that the guaianolides tested were generally more potent activators of Nrf2/ARE in mouse primary cortical cultures then the germacranolides and eudesmanolides tested. Furthermore **10**, which lacked the endoperoxide functionality was the most potent Nrf2/ARE activator and among the least toxic SL. Further structure activity studies with guaianolides may lead to interesting compounds for drug development or biological research tools for studying the Nrf2/ARE pathway. A deeper understanding of the mechanism of SL for Nrf2/ARE activity is also required to determine if SL activity is due to direct binding with cysteine residues on Keap1 or an indirect mechanism such as depletion of glutathione. Finally, whether or not toxicity of SL *in vivo* is a problem should be investigation in more detail as well as toxicity on other cell types.

Acknowledgements

We thank the European Union Seventh Framework Program for funding the Terpmed project of which this research is a part of. Grant number 227448. The work was also funded by R01ES08089 and R01ES10042 from the National Institute of Environmental Health Sciences (JAJ). Finally, we would like to thank Young Hae Choi and the Leiden University Chemistry Department for helping acquire NMR spectra.

Figure 3. Percent Cell viability in MTS assay. *Statistically significant cellular toxicity, $p < 0.05$.

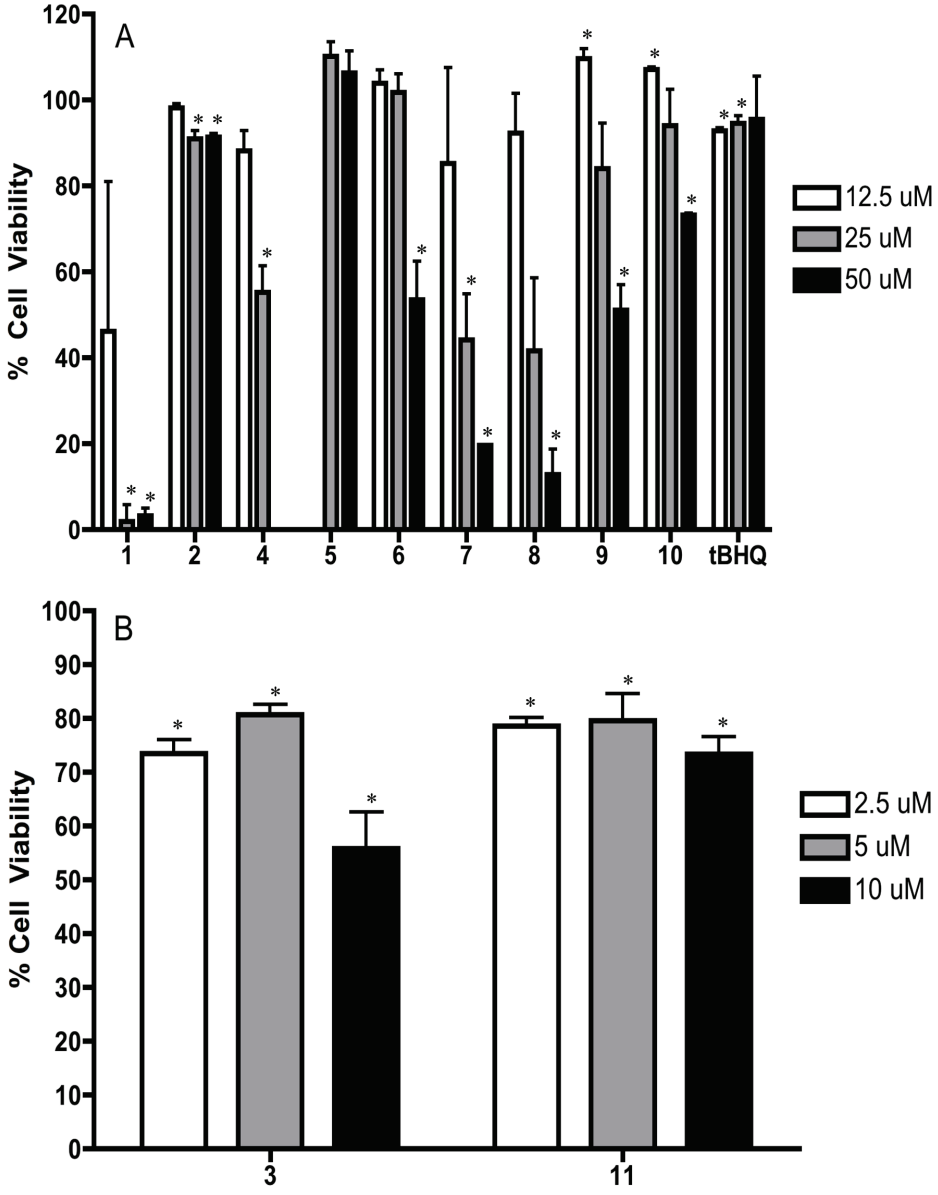

References

Abad, M.J., Bermejo, P., Villar, A., 2006. An approach to the genus Tanacetum L. (Compositae): Phytochemical and pharmacological review. Phytotherapy Research 9, 79–92.

Asakawa, Y., Toyota, M., Takemoto, T., 1981. Two guaiane-type sesquiterpene lactones and their related sesquiterpene lactones from Porella japonica. Phytochemistry 20, 257–261.

Begley, M.J., Hewlett, M.J., Knight, D.W., 1989. Revised structures for guaianolide α-methylenebutyro-lactones from feverfew. Phytochemistry 28, 940–943.

Bohlmann, F., Zdero, C., 1982. Naturally-Occurring Terpene Derivatives .454. Sesquiterpene Lactones and Other Constituents from Tanacetum-Parthenium. Phytochemistry 21, 2543–2549.

Calkins, M.J., Johnson, D.A., Townsend, J.A., Vargas, M.R., Dowell, J.A., Williamson, T.P., Kraft, A.D., Lee, J.-M., Li, J., Johnson, J.A., 2009. The Nrf2/ARE pathway as a potential therapeutic target in neurodegenerative disease. Antioxidants & Redox Signaling 11, 497–508.

Castañeda-Acosta, J., Fischer, N.H., Vargas, D., 1993. Biomimetic transformations of parthenolide. Journal of Natural Products 56, 90–98.

de Vries, H.E., Witte, M., Hondius, D., Rozemuller, A.J.M., Drukarch, B., Hoozemans, J., van Horssen, J., 2008. Nrf2-induced antioxidant protection: a promising target to counteract ROS-mediated damage in neurodegenerative disease? Free Radical Biology & Medicine 45, 1375–1383.

El-Feraly, S., Chan, Y.-M., Fairchild, E.H., Doskotch, R.W., 1977. Peroxycostunolide and peroxyparthenolide: two cytotoxic germacranolide hydroperoxides from magnolia grandiflora. Structural revision of verlotorin and artemorin. Tetrahedron Letters 18, 1973–1975.

El-Feraly, F.S., Chan, Y.M., 1978. Isolation and characterization of the sesquiterpene lactones costunolide, parthenolide, costunolide diepoxide, santamarine, and reynosin from Magnolia grandiflora L. Journal of Pharmaceutical Sciences 67, 347–350.

Foucault, A.P., 1995. Centrifugal Partition Chromatography. Marcel Dekker Inc, New York.

Geissman, T.A., 1970. Sesquiterpene lactones of Artemisia— A. verlotorum and A. vulgaris. Phytochemistry 9, 2377–2381.

Ghantous, A., Gali-Muhtasib, H., Vuorela, H., Saliba, N.A., Darwiche, N., 2010. What made sesquiterpene lactones reach cancer clinical trials? Drug Discovery Today 15, 668–678.

Hwang, D.-R., Wu, Y.-S., Chang, C.-W., Lien, T.-W., Chen, W.-C., Tan, U.-K., Hsu, J.T.A., Hsieh, H.-P., 2006. Synthesis and anti-viral activity of a series of sesquiterpene lactones and analogues in the subgenomic HCV replicon system. Bioorganic & Medicinal Chemistry 14, 83–91.

Itoh, K., Tong, K.I., Yamamoto, M., 2004. Molecular mechanism activating Nrf2-Keap1 pathway in regulation of adaptive response to electrophiles. Free Radical Biology & Medicine 36, 1208–1213.

Jeong, W.-S., Keum, Y.-S., Chen, C., Jain, M.R., Shen, G., Kim, J.-H., Li, W., Kong, A.-N.T., 2005. Differential expression and stability of endogenous nuclear factor E2-related factor 2 (Nrf2) by natural chemopreventive compounds in HepG2 human hepatoma cells. Journal of Biochemistry and Molecular Biology 38, 167–176.

Johnson, D.A., Andrews, G.K., Xu, W., Johnson, J.A., 2002. Activation of the antioxidant response element in primary cortical neuronal cultures derived from transgenic reporter mice. Journal of Neurochemistry 81, 1233–1241.

Kim, S.-K., Cho, S.-B., Moon, H.-I., 2010. Neuroprotective effects of a sesquiterpene lactone and flavanones from Paulownia tomentosa Steud. against glutamate-induced neurotoxicity in primary cultured rat cortical cells. Phytotherapy Research 24, 1898–1900.

Kraft, A.D., Johnson, D.A., Johnson, J.A., 2004. Nuclear factor E2-related factor 2-dependent antioxidant response element activation by tert-butylhydroquinone and sulforaphane occurring preferentially in astrocytes conditions neurons against oxidative insult. Journal of Neuroscience 24, 1101–1112.

Majdi, M., Liu, Q., Karimzadeh, G., Malboobi, M.A., Beekwilder, J., Cankar, K., de Vos, R., Todorovic, S., Simonovic, A., Bouwmeester, H., 2011. Biosynthesis and localization of parthenolide in glandular trichomes of feverfew (Tanacetum parthenium L. Schulz Bip.). Phytochemistry 72, 1739–1750.

Mathema, V.B., Koh, Y.-S., Thakuri, B.C., Sillanpää, M., 2012. Parthenolide, a sesquiterpene lactone, expresses multiple anti-cancer and anti-inflammatory activities. Inflammation 35, 560–565.

Milbrodt, M., Schröder, F., König, W.A., 1997. 3,4-β-Epoxy-8-deoxycumambrin B, A sesquiterpene lactone from Tanacetum parthenium. Phytochemistry 44, 471–474.

Neukirch, H., Kaneider, N.C., Wiedermann, C.J., Guerriero, A., D'Ambrosio, M., 2003. Parthenolide and its photochemically synthesized 1(10)Z isomer: chemical reactivity and structure–activity relationship studies in human leucocyte chemotaxis. Bioorganic & Medicinal Chemistry 11, 1503–1510.

Parodi, F.J., Fronczek, F.R., Fischer, N.H., 1989. Biomimetic Transformations of 11,13-Dihydroparthenolide and Oxidative Rearrangements of a Guai- 1(10)-en-6,12-olide. Journal of Natural Products 52, 554–566.

Rey, J.-P., Levesque, J., Louis Pousset, J., 1992. Extraction and high-performance liquid chromatographic methods for the γ-lactones parthenolide (Chrysanthemum parthenium Bernh.), marrubiin (Marrubium vulgare L.) and artemisinin (Artemisia annua L.). Journal of Chromatography A 605, 124–128.

Romo de Vivar, A., Jiménez, H., 1965. Structure of santamarine, a new sesquiterpene lactone. Tetrahedron 21, 1741–1745.

Salminen, A., Lehtonen, M., Suuronen, T., Kaarniranta, K., Huuskonen, J., 2008. Terpenoids: natural inhibitors of NF-kappaB signaling with anti-inflammatory and anticancer potential. Cellular and Molecular Life Sciences 65, 2979–2999.

Sanz, J.F., Barbera, O., Marco, J.A., 1989. Sesquiterpene lactones from Artemisia hispanica. Phytochemistry 28, 2163–2167.

Tiuman, T.S., Ueda-Nakamura, T., Garcia Cortez, D.A., Dias Filho, B.P., Morgado-Díaz, J.A., De Souza, W., Nakamura, C.V., 2005. Antileishmanial Activity of Parthenolide, a Sesquiterpene Lactone Isolated from Tanacetum Parthenium. Antimicrobial Agents and Chemotherapy 49, 176–182.

Tukov, F.F., Anand, S., Gadepalli, R.S.V.S., Gunatilaka, A.A.L., Matthews, J.C., Rimoldi, J.M., 2004. Inactivation of the cytotoxic activity of repin, a sesquiterpene lactone from Centaurea repens. Chemical Research in Toxicology 17, 1170–1176.

Umemura, K., Itoh, T., Hamada, N., Fujita, Y., Akao, Y., Nozawa, Y., Matsuura, N., Iinuma, M., Ito, M., 2008. Preconditioning by sesquiterpene lactone enhances H2O2-induced Nrf2/ARE activation. Biochemical and Biophysical Research Communications 368, 948–954.

Yoshioka, H., Renold, W., Fischer, N.H., Higo, A., Mabry, T.J., 1970. Sesquiterpene lactones from Ambrosia confertiflora (Compositae). Phytochemistry 9, 823–832.

Zhang, D.D., Hannink, M., 2003. Distinct cysteine residues in Keap1 are required for Keap1-dependent ubiquitination of Nrf2 and for stabilization of Nrf2 by chemopreventive agents and oxidative stress. Molecular and Cellular Biology 23, 8137–8151.

Appendix Chapter 5

Tanacetum parthenium (IBRSS) growth conditions

The seeds stock (Item No. CA474) was purchased from Jelitto Trade Company GmbH (Schwarmstedt, Germany). Seeds were germinated in the greenhouse on FLORADUR Fine soil seed starting mixture (*Floragard*, Vertriebs GmbH, Oldenburg, Germany), under long day conditions, 16 h light and 8 h darkness. Four week old seedlings were transferred to FLORADUR B soil (*Floragard*, Vertriebs GmbH, Oldenburg, Germany), in separate pots. After 2 months seedlings were transferred from the greenhouse to an open-air garden. After several days adaptation to the open air environmental conditions seedlings were planted in the cultivation field. Plants were grown from spring to autumn 2010. During flowering time, flowers were subsequently harvested and dried at the room temperature.

Table A1. ^{1}H-NMR data ($CDCl_3$, 500 MHz)

	Parthenolide	**11,13-Dihydroparthenolide**	**3-Hydroxyparthenolide**
H-1	5.21 br dd (2.6, 12.1)	5.17 br dd (2.3, 12.2)	5.14 br dd (4, 12)
H-2α	2.12-2.23 m	2.11-2.21 m	2.35-2.52 m
H-2β	2.35-2.46 m	2.34-2.44 m	2.35-2.52 m
H-3α	1.20-1.28 m	1.22 td (5.7, 12.9)	3.43 dd (7, 11)
H-3β	2.12-2.23 m	2.11-2.21 m	
H-5	2.78 d (8.9)	2.70 d (9)	2.79 d (9)
H-6	3.86 t (8.6)	3.81 t (9.1)	3.92 t (9)
H-7	2.76-2.81 m	1.81-1.93 m	2.74 ddddd (3, 4, 6, 9, 9)
H-8α	2.12-2.23 m	1.81-1.93 m	2.53-2.52 m
H-8β	1.69-1.77 m	1.61-1.69 m	1.68 m
H-9α	2.12-2.23 m	2.05 br t (12.5)	2.13 m
H-9β	2.35-2.46 m	2.25-2.34 m	2.35-2.52 m
H-11		2.25-2.34 m	
H-13α	6.34 d (3.7)		6.34 d (4)
H-13β	5.62 d (3.3)	1.28 d (7.2)	5.63 d (3)
H-14	1.72 br s	1.7 br s	1.73 s
H-15	1.31 s	1.29 s	1.32 s

Table A2. ^{1}H-NMR data ($CDCl_3$, 500 MHz)

	3β-Hydroxycostunolide	**Costunolide diepoxide**
H-1	4.90 br dd (2.9, 12)	2.85 dd (1, 11)
H-2α	2.41-2.48 m	1.51 tdd (5, 11, 14, 14)
H-2β	2.28 td (10.3, 12, 12.1)	2.16-2.3 m
H-3α	4.28 m	1.20-1.29 m
H-3β		2.48 dd (8, 14)
H-5	4.79 br d (9.9)	2.91 d (9)
H-6	4.61 dd (8.7, 9.9)	3.94 t (9)
H-7	2.53 m	2.73 tq (3, 3, 3, 9, 9)
H-8α	2.06-2.13 m	1.20-1.29 m
H-8β	1.65-1.73 m	1.61 m
H-9α	2.41-2.48 m	2.16-2.30 m
H-9β	2.06-2.13 m	2.16-2.30 m
H-13α	6.29 d (3.6)	6.34 d (4)
H-13β	5.54 d (3.2)	5.62 d (3)
H-14	1.46 br s	1.40-1.35*
H-15	1.74 d (1.4)	1.40-1.35*

*Interchangeable

Table A3. ^{1}H-NMR data ($CDCl_3$, 500 MHz)

	Anhydroverlotorin	**Artemorin***
1α		3.96 br
H-2α	2.34-2.65 m	1.9-2.9 br m
H-2β	3.15 br m	1.9-2.9 br m
H-3α	2.34-2.65 m	1.9-2.9 br m
H-3β	2.34-2.65 m	1.9-2.9 br m
H-5	5.09 br d (10)	5.22 br d (10)
H-6	4.33 t (10)	4.39 br
H-7	2.56 m	2.75 m
H-8α	2.26 m	1.9-2.9 br m
H-8β	1.41 m	1.9-2.9 br m
H-9α	2.33-2.62 m	1.9-2.9 br m
H-9β	2.33-2.62 m	1.9-2.9 br m
H-13α	6.22 d (3.5)	6.16 d (3)
H-13β	5.48 d (3.2)	5.44 d (3)
H-14	5.48 s	5.20 br s
H-14	5.66 s	4.86 br s
H-15	1.75 d (1)	1.71 br s

*Peak broadening

Table A4. ^{1}H-NMR data ($CDCl_3$, 500 MHz)

	Santamarine	Reynosin
H-1α	3.68 ddd (5, 5, 10)	3.53 dd (5, 11)
H-2α	2.4 dddd (3, 5, 10, 16)	1.50-1.88 m*
H-2β	1.97 ddd (3, 10, 17)	1.50-1.88 m*
H-3	5.34 m	2.04-2.16 m
H-3		2.34 ddd (2, 5, 14)
H-5	2.35 br d (11)	2.19 br dd (2, 11)
H-6	3.95 t (11)	4.03 t (11)
H-7	2.50 ddddd (3, 3, 3, 10, 14)	2.54 m
H-8	1.65 qd (3, 13.5, 14, 14)	2.04-2.16 m
H-8	2.02-2.13 m	1.50-1.88 m*
H-9	1.31 td (4, 13, 13)	1.32-1.40 m*
H-9	2.02-2.13 m	2.04-2.16 m
H-13α	6.08 d (3)	6.09 d (3)
H-13β	5.41 d (3)	5.41 d (3)
H-14	0.88 s	0.82 s
H-15	1.83 br s	4.99 d (1)
H-15		4.87 d (1)

*Signals obscured by H_2O

Table A5. ^{1}H-NMR data ($CDCl_3$, 500 MHz)

	Tanaparthin-β-peroxide	**Artecanin**
H-2	6.33 d (6)	3.55 d (1)
H-3	6.29 d (6)	3.30 d (1)
H-5	2.65 d (10)	2.86 d (11)
H-6	3.75 t (10)	4.09 t (11)
H-7	3.36 ddddd (3, 3.5, 7, 10, 10)	3.26-3.33 m
H-8	1.52*	1.64-2.13
H-8	2.36 dddd (7, 9, 10, 14)	1.64-2.13
H-9	1.74 m	1.64-2.13
H-9	2.03 ddd (2, 8, 16)	1.64-2.13
H-13α	6.15 d (3.5)	6.20 d (3.5)
H-13β	5.42 d (3)	5.43 d (3)
H-14	1.39 s	1.14 s
H-15	1.71 s	1.56 s

*Signals obscured by H_2O

Table A6. High resolution MS data

Number	compound name	observed $[M+H]^+$	calculated [M+H]+	Formula	Δ ppm
1	parthenolide	249.1489	249.1485	$C_{15}H_{20}O_3$	1.69
2	11,13-dihydroparthenolide	251.1644	251.1642	$C_{15}H_{22}O_3$	1.04
3	anhydroverlotorin	247.1332	247.1329	$C_{15}H_{18}O_3$	1.38
4	santamarine	249.1488	249.1485	$C_{15}H_{20}O_3$	1.08
5	reynosin	249.1487	249.1485	$C_{15}H_{20}O_3$	0.84
6	3β-hydroxycostunolide	249.1487	249.1485	$C_{15}H_{20}O_3$	0.72
7	costunolide diepoxide	265.1435	265.1434	$C_{15}H_{20}O_4$	0.30
8	3-hydroxyparthenolide	265.1436	265.1434	$C_{15}H_{20}O_4$	0.68
9	artemorin	249.1486	249.1485	$C_{15}H_{20}O_3$	0.16
10	artecanin	279.1228	279.1227	$C_{15}H_{18}O_5$	0.25
11	tanaparthin-β-peroxide	279.1226	279.1227	$C_{15}H_{18}O_5$	-0.29

Figure A1. Parthenolide ^{1}H-NMR.

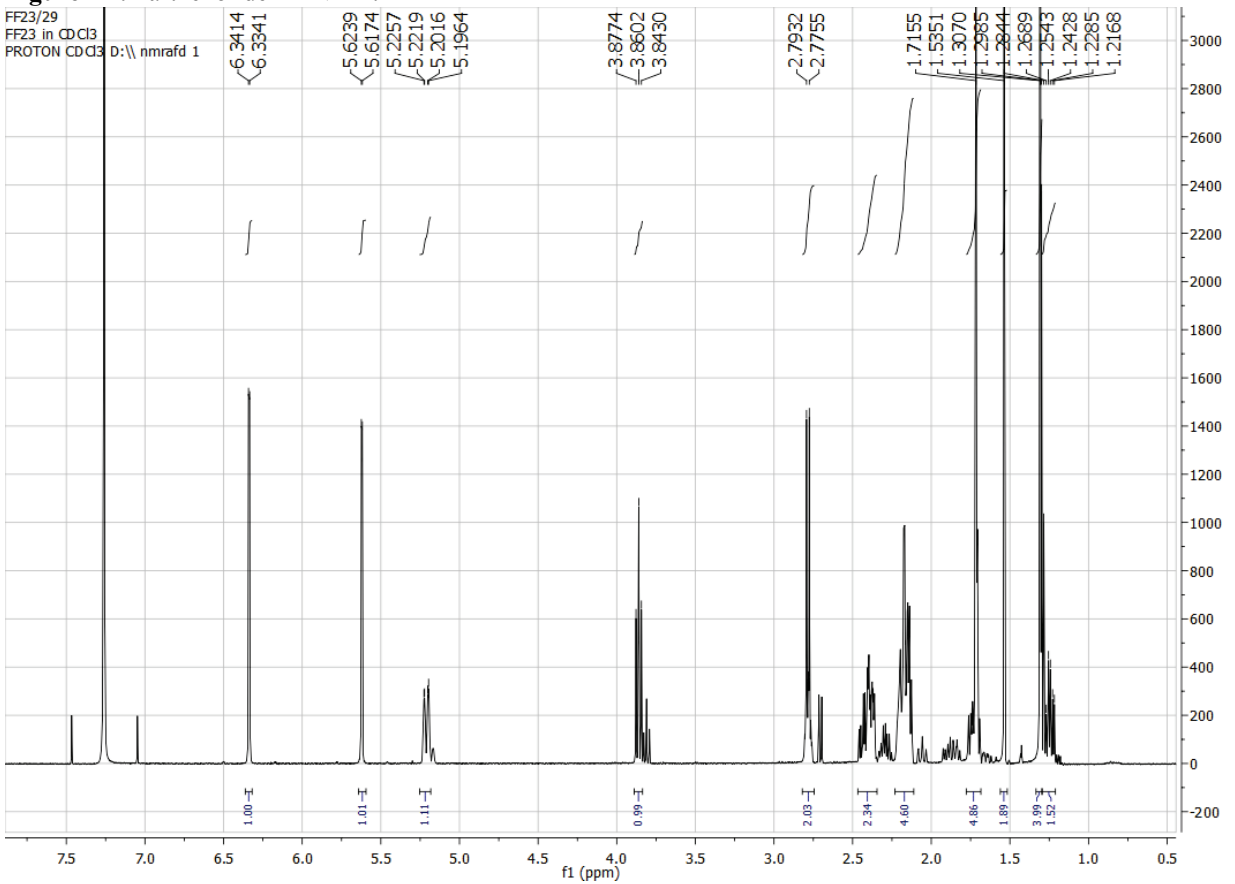

Figure A2. 11,13-Dihydroparthenolide ^{1}H-NMR.

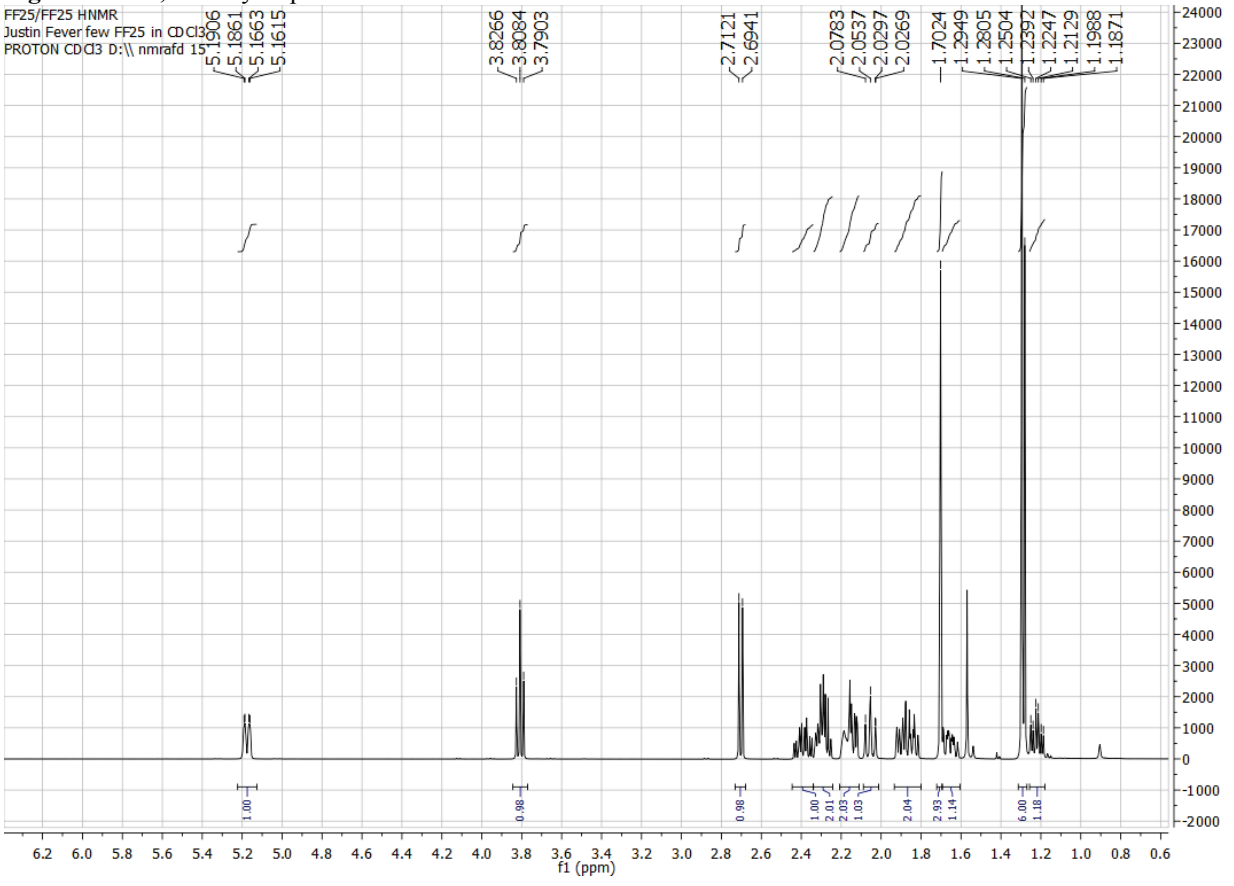

Figure A3. 3-Hydroxyparthenolide ^{1}H-NMR.

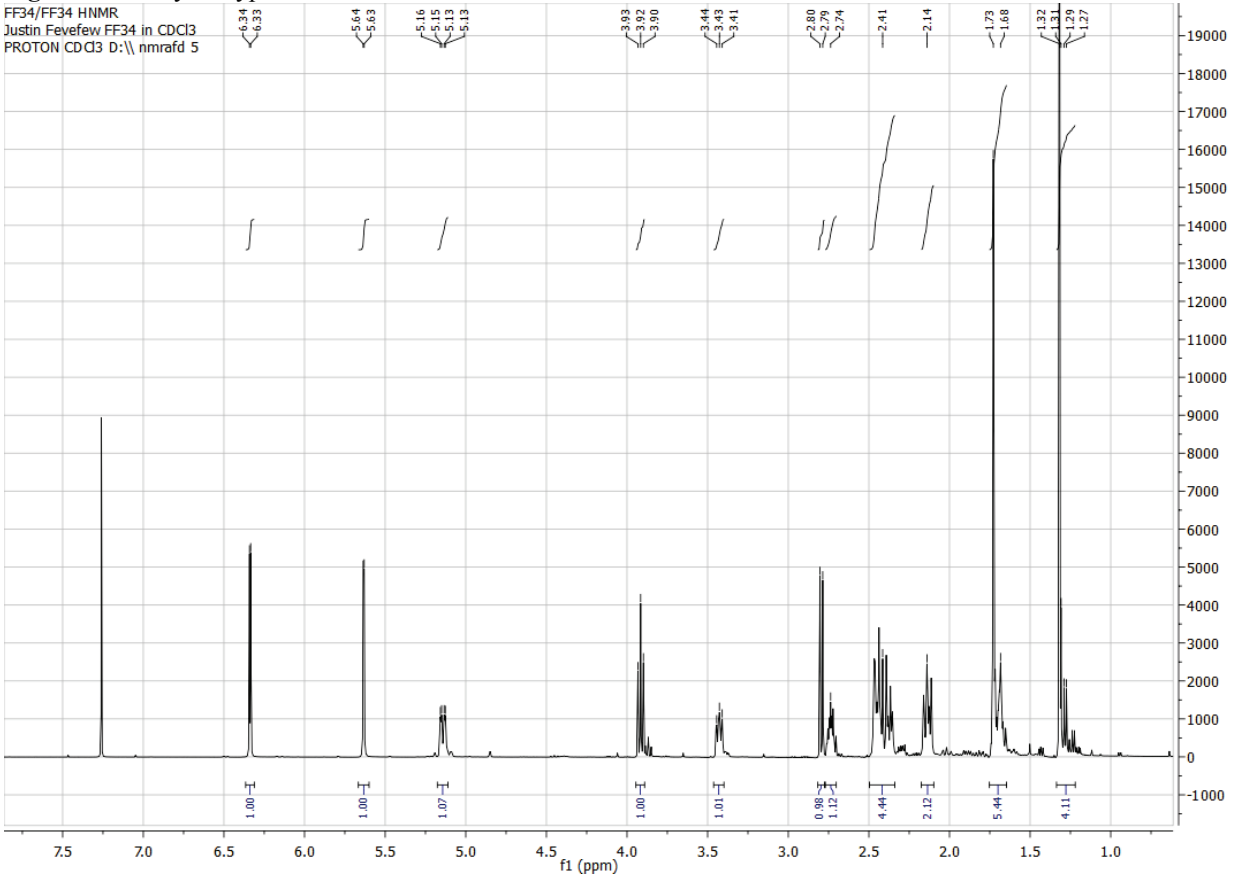

Figure A4. 3β-Hydoxycostunolide ^{1}H-NMR.

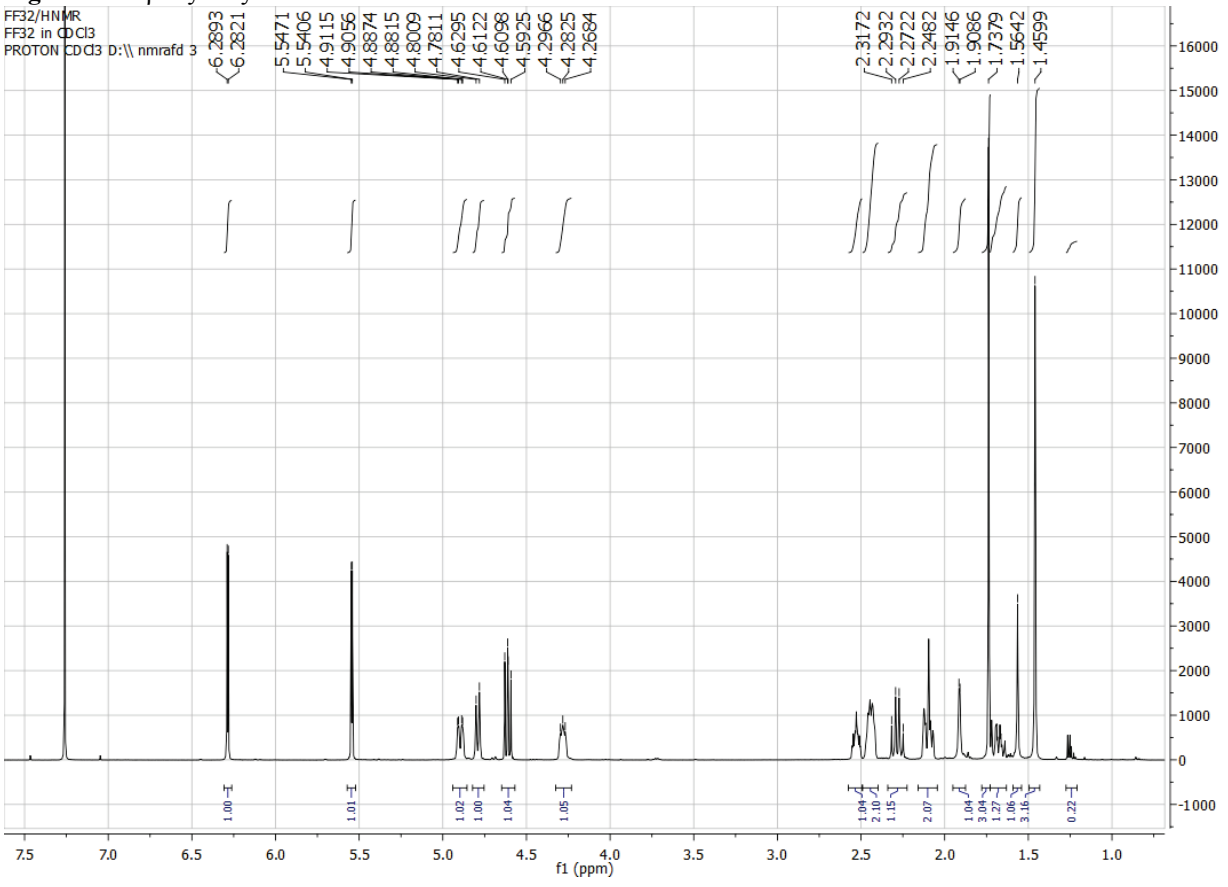

Figure A5. Costunolide diepoxide ^{1}H-NMR.

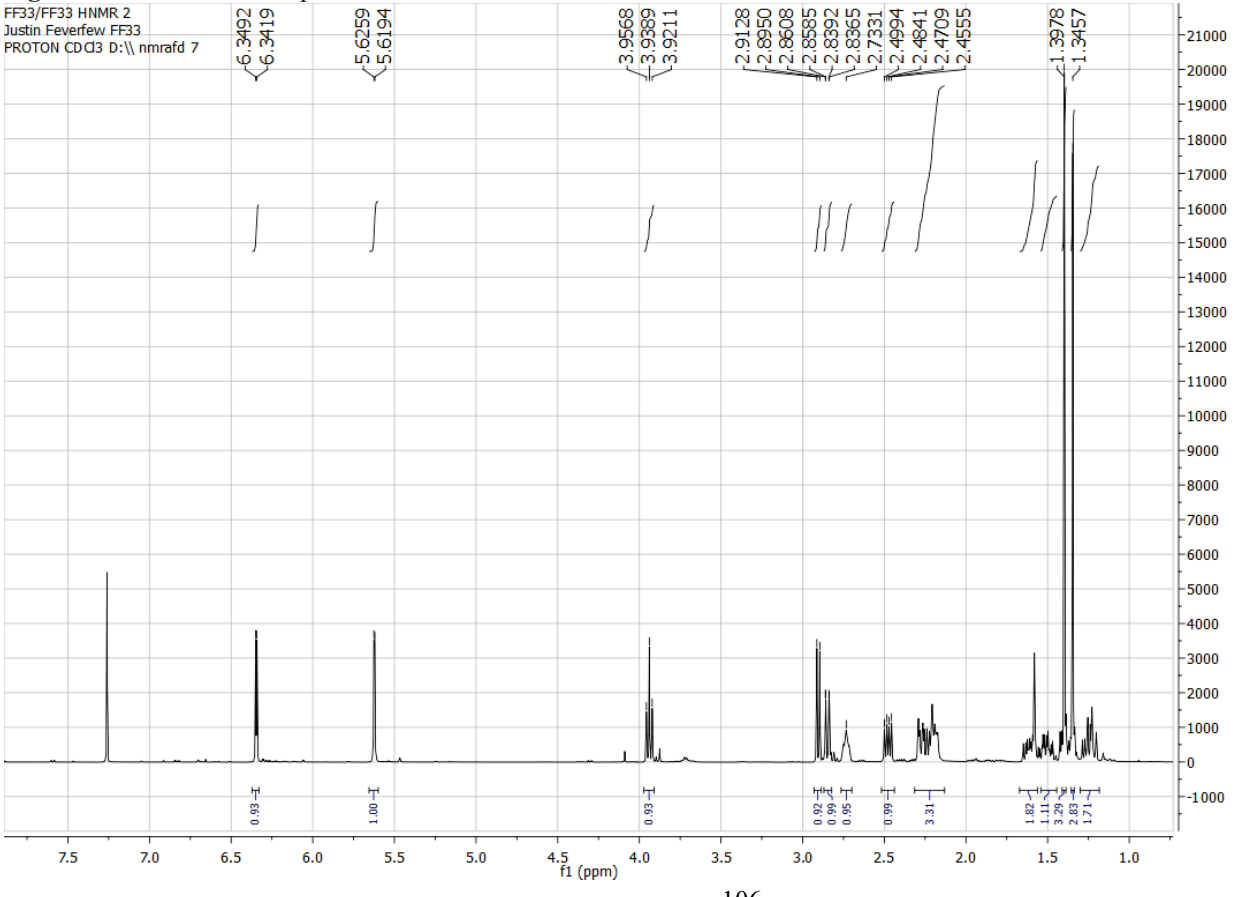

Figure A6. Anhydroverlotorin ^{1}H-NMR.

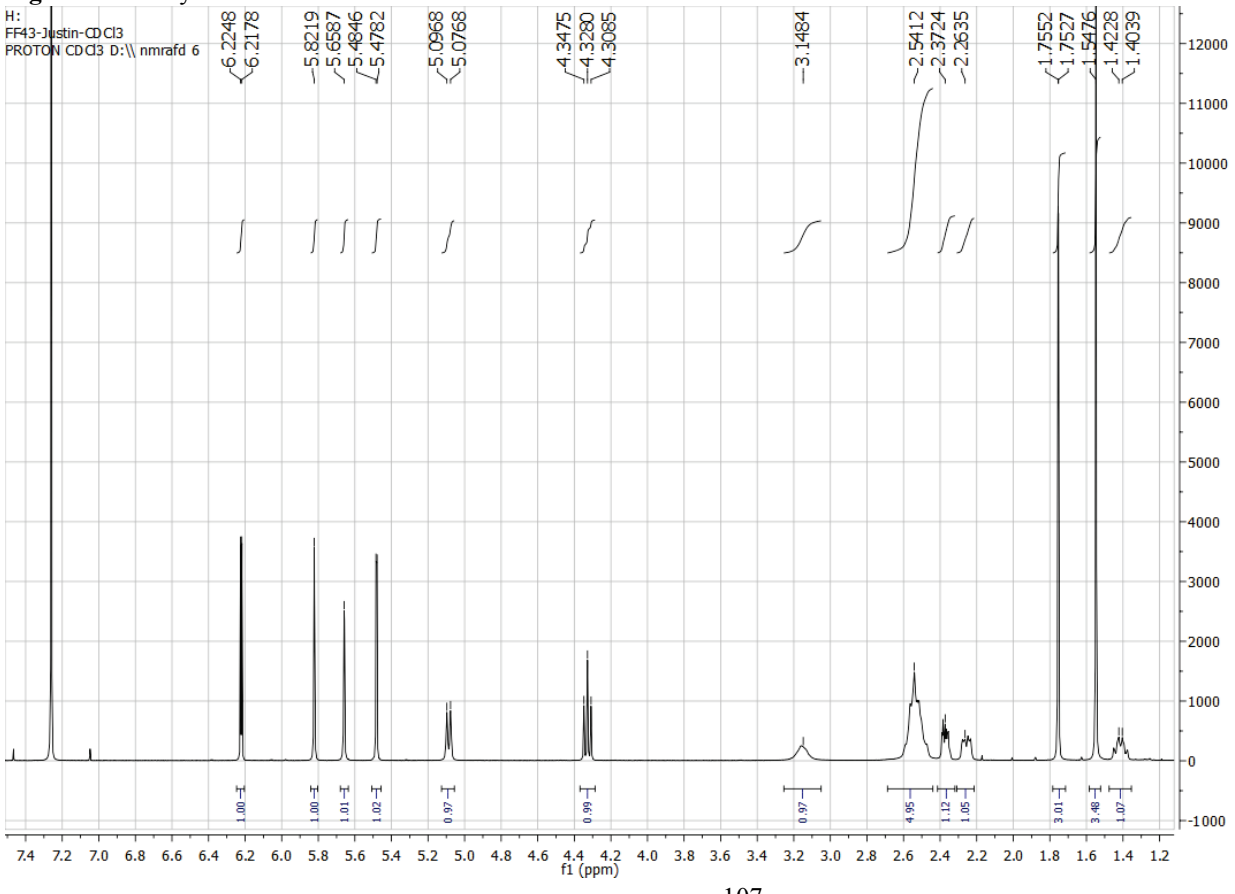

Figure A7. Artemorin ^{1}H-NMR.

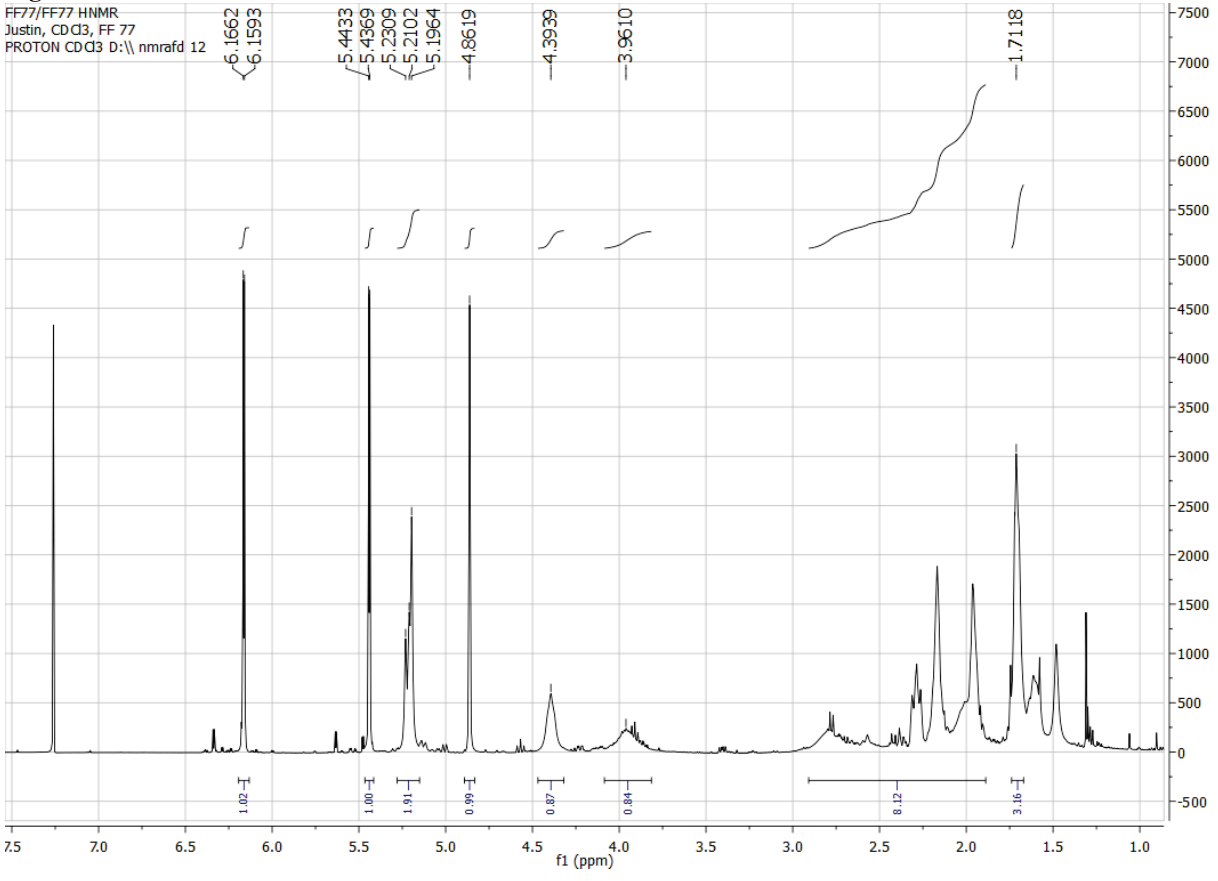

Figure A8. Santamarine ^{1}H-NMR.

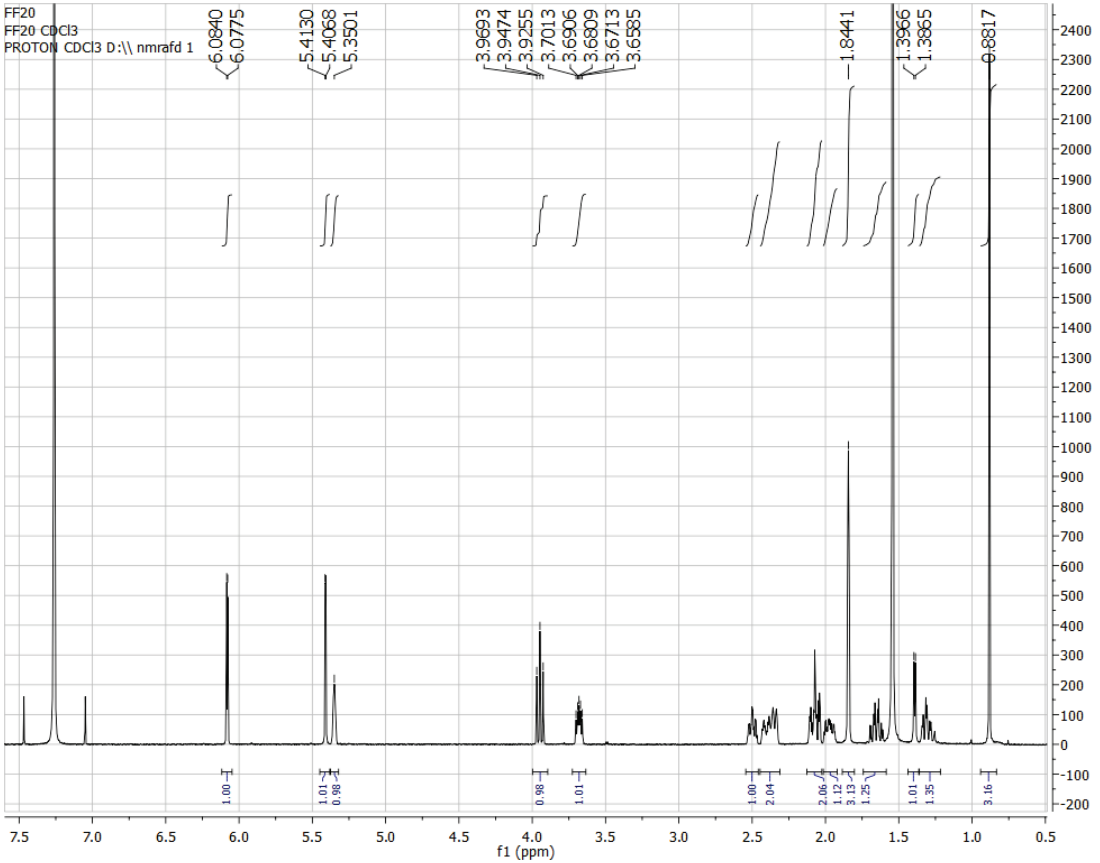

Figure A9. Reynosin ^{1}H-NMR

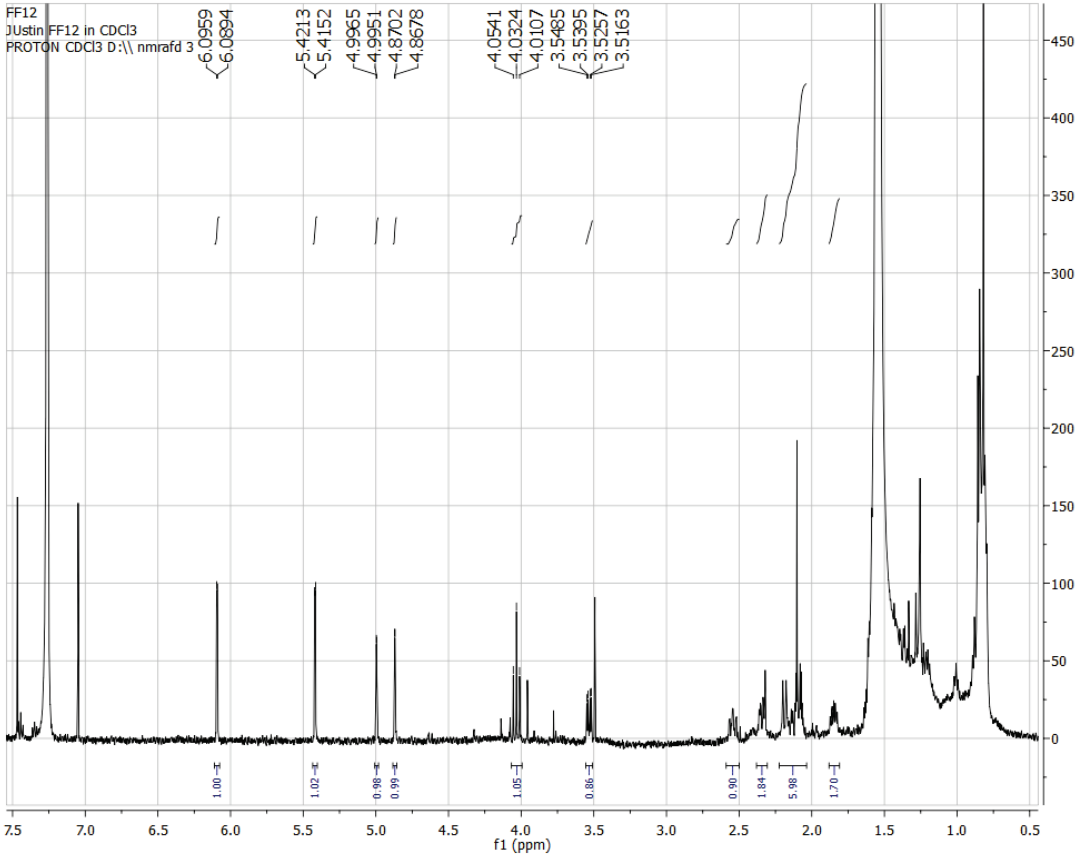

Figure A10. Tanaparthin-β-peroxide ^{1}H-NMR

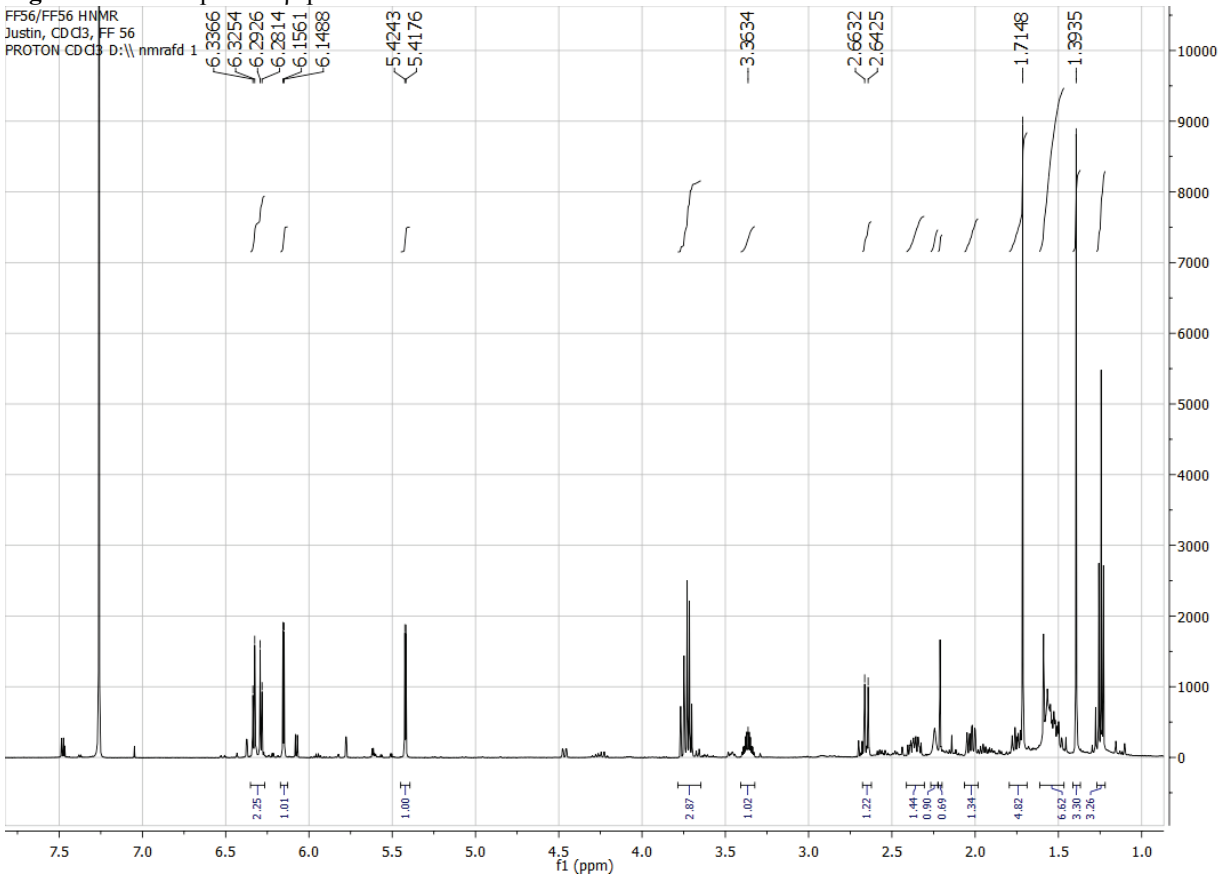

Figure A11. Artecanin ^{1}H-NMR